AJNR

Diffuse Axonal Injury Associated with Chronic Traumatic Brain Injury: Evidence from T2*-weighted Gradient-echo Imaging at 3 T

Rainer Scheid, Cristoph Preul, Oliver Gruber, Christopher Wiggins and D. Yves von Cramon

AJNR Am J Neuroradiol 2003, 24 (6) 1049-1056
http://www.ajnr.org/content/24/6/1049

AJNR Am J Neuroradiol 24:1049–1056, June/July 2003

Diffuse Axonal Injury Associated with Chronic Traumatic Brain Injury: Evidence from T2*-weighted Gradient-echo Imaging at 3 T

Rainer Scheid, Cristoph Preul, Oliver Gruber, Christopher Wiggins, and D. Yves von Cramon

BACKGROUND AND PURPOSE: **Diffuse axonal injury is frequently accompanied by tissue tear hemorrhages. We examined whether high field strength T2*-weighted gradient-echo imaging performed during the chronic stage of traumatic brain injury may have advantages in the evaluation of diffuse axonal injury as compared with T1- and T2-weighted MR imaging.**

METHODS: **Prospective MR imaging of 66 patients (age range, 17–57 years) was performed using a 3-T system 3 to 292 months (median, 23.5 months) after traumatic brain injury. T1-, T2-, T2*-hypointense and T2-hyperintense foci of 1- to 15-mm diameter were registered in 10 brain regions by two readers separately. Foci that appeared hypointense both on the T1- and T2- and/or on the T2*-weighted images were defined as traumatic microbleeds.**

RESULTS: **For 46 (69.7%) of the patients, T2*-weighted gradient-echo imaging revealed traumatic microbleeds. Hyperintense foci were observed on the T2-weighted images of only 15 (22.7%) patients. T2*-weighted imaging showed significantly more traumatic microbleeds ($P = .000$) than did T1- and T2-weighted imaging. Interobserver agreement was strong ($\kappa = 0.79$, $\tau = 0.749$, $P = .000$). For 14 (21.2%) of the patients, T2*-weighted gradient-echo imaging revealed traumatic microbleeds in the corpus callosum, whereas for only two (3%), hyperintense callosal lesions were seen on the T2-weighted images. Although a significant correlation existed between the total amount and callosal appearance of traumatic microbleeds and Glasgow Coma Scale scores ($P = .000$), no correlation existed with extended Glasgow Outcome Scale scores.**

CONCLUSION: **T2*-weighted gradient-echo imaging at high field strength is a useful tool for the evaluation of diffuse axonal injury during the chronic stage of traumatic brain injury. Diffuse axonal injury-related brain lesions are mainly hemorrhagic. The relevance of diffuse axonal injury for long-term clinical outcome is uncertain.**

T2*-weighted gradient-echo MR imaging is known to be highly sensitive for detecting brain hemorrhage (1–3). Magnetic susceptibility differences resulting from the presence of paramagnetic blood breakdown products create local magnetic field inhomogeneities, which manifest as marked hypointensity on T2*-images (1, 3–5). The T2* signal intensity loss is greater with higher magnetic field strength (1, 6, 7), which makes the use of the sequence at 3 T practical. Only a few reports are presented in the literature in which T2*-weighted gradient-echo imaging has been used in the investigation of traumatic brain injury (6, 8, 9). Yanagawa et al (9) presented what, to our knowledge, is the only study that directly compares T2- and T2*-weighted gradient-echo imaging of traumatic brain injury. They found T2*-weighted gradient-echo imaging to be useful for evaluating the clinical symptoms of head injury during the acute stage of the disease. Information regarding its usefulness during the chronic stage is lacking.

Diffuse axonal injury is a specific type of primary traumatic brain injury (10–19). Although evidence exists in the neuropathologic literature that diffuse axonal injury is typically accompanied by small hemorrhages, or so-called *tissue tear hemorrhages* (10, 11, 13, 19), almost all previous MR imaging studies of traumatic brain injury state that most diffuse axonal injury lesions are nonhemorrhagic (6, 8, 20–24). However, in the study presented by Yanagawa et al

Received October 22, 2002; accepted after revision, December 26.

Presented in part at the annual meeting of the Deutsche Gesellschaft für Neurologie, Mannheim, Germany, September 2002.

From the Day Clinic of Cognitive Neurology (R.S., D.Y.v.), University of Leipzig, Leipzig, Germany; the Max-Planck-Institute of Cognitive Neuroscience (R.S., C.P., O.G., C.W., D.Y.v.C.), Leipzig, Germany; the Department of Psychiatry (O.G.), University of Ulm, Ulm, Germany; and the MGH-NMR Center (C.W.), Massachusetts General Hospital, Charlestown, MA.

Address reprint requests to Dr. Rainer Scheid, Day Clinic of Cognitive Neurology, University of Leipzig, Liebigstr. 22a, 04103 Leipzig, Germany.

(9), a high number of hemorrhagic (ie, T2* hypointense) lesions were reported.

Our aim was to study the usefulness of T2*-weighted gradient-echo imaging at high field strength for the evaluation of diffuse axonal injury during the chronic stage of traumatic brain injury and to clarify the neuroradiologic appearance of diffuse axonal injury-related lesions. In clinical circumstances, it is often asked whether a certain symptom or syndrome (often neuropsychologic and/or behavioral) might be due to brain injury if the patient has a history of head injury. In particular, our hypotheses were as follows: 1) not just during the acute stage but also during the chronic stage of traumatic brain injury, T2*-weighted gradient-echo imaging shows more focal traumatic lesions other than focal cortical contusions than do T1- and T2-weighted MR imaging; 2) localization and number of diffuse axonal injury-related lesions correlate with clinical scores of injury severity (Glasgow Coma Scale [GCS]) (25) and outcome (extended Glasgow Outcome Scale [GOS]) (26).

Methods

Sixty-six patients (15 women, 51 men) with histories of traumatic brain injury were prospectively studied between September 2000 and September 2001. All patients were in-patients of the Day Clinic of Cognitive Neurology, University of Leipzig. Patients' ages ranged from 17 to 57 years (median, 33 years). All participants provided written informed consent.

Clinical information was collected to establish the following parameters: type of head injury (open or closed), multiple injuries, cause of injury (traffic accident, fall, assault/blow), history of arterial hypertension, diabetes mellitus, stroke, chronic alcohol abuse, previous traumatic brain injury, other chronic medical problems, and time interval between traumatic brain injury and MR imaging. Injury severity was assessed by depth of initial coma, by using the reported GCS score. In cases in which information regarding GCS score was missing (n = 43), specific information from the acute records was used to calculate GCS scores retrospectively. Because the GCS score is strictly descriptive, this reconstruction is adequate (27). For four patients, the GCS score could not be calculated because of insufficient information. Because of the interference of standard therapeutic interventions, length of coma is not reported. Overall functional outcome was assessed by using the extended GOS not before 6 months after traumatic brain injury (26).

MR imaging was performed on a 3-T whole body system (Medspec 3T/100; Bruker, Ettlingen, Germany). The imaging protocol consisted of three imaging sessions of the same geometry (20 sections; axial plane; section thickness, 5 mm; section gap, 2 mm): 1) 2D T1-weighted reduced power multisection modified driven equilibrium Fourier transform imaging (28) (1.3/10 [TR/TE]; field of view, 25.0 × 25.0 cm; data matrix, 256 × 256), using non-section-selective inversion pulse and then a single excitation of each section to reduce the amount of RF power; 2) 2D T2-weighted fast spin-echo imaging (8.5/21.7; field of view, 25.0 × 25.0 cm; data matrix, 512 × 512); and 3) 2D T2*-weighted gradient-echo imaging (700/15; field of view, 19.2 × 19.2 cm; data matrix, 256 × 256; flip angle, 25 degrees).

Any small (1–15 mm) focus without connection to the brain surface and/or the ventricular system that appeared hypointense on T1- and T2- and/or T2*-weighted gradient-echo MR images was defined as a traumatic microbleed. Overlap with vascular structures was avoided. Areas of symmetric hypointensity of the globus pallidus, likely to represent calcification, were disregarded. To exclude focal cortical contusions and considering the pathogenesis of diffuse axonal injury, extensive foci (>15 mm) and foci in contact with the brain surface were excluded. In addition, every T2-hyperintense signal intensity of the same size was registered. The total number of lesions was counted for each sequence and was divided into the following 10 brain regions: frontal lobe, temporal lobe, parietal lobe, occipital lobe, cerebellum, basal ganglia, thalamus, corpus callosum, midbrain, and brain stem. Additionally, the following data were collected: focal cortical contusion, extensive traumatic hemorrhage, gliding contusion, ischemic brain lesion, and residue from brain surgery. The occurrence of brain atrophy and hydrocephalus (which, because of the lack of accepted common criteria, was evaluated according to the subjective concordant judgment of two separate investigators) as possible long-term residues of traumatic brain injury was noted. Because cerebral microangiopathy is known to cause cerebral microbleeds (5, 29–34), the readers were aware for signs of leukoaraiosis and lacunar infarcts.

Images were evaluated independently by two neuroradiology expert readers (R.S., C.P.), one of whom was blinded to the clinical data. Statistical analysis was conducted by using the coefficient of agreement of Cohen and nonparametric statistics (Wilcoxon matched-pairs signed rank test, Kendall rank correlation, Spearman rank correlation, Mann-Whitney U test, Kruskall-Wallis analysis of variance). After correction for multiple comparisons, values of $P < .01$ and $P < .005$ were considered significant.

TABLE 1: Clinical data

	Number or Range	Median	Percent
n	66		
Age (yr)	17–57	33	
Sex			
Male	51		77.3
Female	15		22.7
Time interval			
TBI–MR imaging (mo)	3–292	23.5	
Type of head injury			
Open	17		25.8
Closed	49		74.2
Cause of injury			
Traffic accident	45		68.2
Fall	16		24.2
Blow/assault	5		7.6
Multiple injuries	9		13.6
Medical history			
Hypertension	1		1.5
Diabetes mellitus	0		0
Lacunar stroke	0		0
Alcohol abuse	3		4.5
TBI	2		3
GCS score (n = 62)	3–15	6	
GOS score	3–8	5	

Note.—TBI indicates traumatic brain injury; GCS, Glasgow Coma Scale; GOS, Glasgow Outcome Scale.

Results

Patients

Patients' clinical and demographic data are shown in Table 1. Because of the observation of microbleeds in participants with vascular risk factors (29, 34), it is of special importance that only one patient had a history of chronic arterial hypertension and that none had a history of diabetes mellitus or stroke, especially lacunar stroke. Two participants had histories of multiple traumatic brain injuries.

TABLE 2: Frequency of focal lesions

	Total Lesions	Range	Median ± SD
T1	326	0–31	2.5 ± 6.8*
T2 hypo	168.5	0–12	1.0 ± 3.6*
T2 hyper	65	0–10	0 ± 2.25*
T2*	608	0–61	3.75 ± 13.9

Note.—T1 indicates T1-weighted MR imaging; T2 hypo, T2-weighted MR imaging hypointensities; T2 hyper, T2-weighted MR imaging hyperintensities; T2*, T2*-weighted MR imaging.

MR Imaging Results

The MR imaging results are summarized in Table 2. For nine (13.6%) patients, MR imaging was without any pathologic results. With respect to traumatic microbleeds, for 20 (30.3%) patients, MR imaging was negative in all sequences. For 22 (33.3%) patients, T1-weighted MR imaging was negative, and for 25 (37.9%) patients, T2-weighted MR imaging was negative. Traumatic microbleeds most commonly measured 1- to 5-mm in diameter. The grand total of lesions found by the two separate readers (across participants) and the number of lesions per patient were significantly greater on the T2*-weighted images (608 total lesions; median, 3.75 lesions; range, 0–61 lesions) than on the T1-weighted images (326 total lesions; median, 2.5 lesions; range, 0–31 lesions) or the T2-weighted images (168.5 total lesions; median, 1.0 lesions; range, 0–12 lesions) (Wilcoxon matched-pairs signed rank test, $P = .0000$). Interobserver agreement regarding the presence of traumatic microbleeds was strong ($\kappa = 0.79$) (35, 36). To verify inter-rater agreement for every participant, the rank correlation τ of Kendall (37) was used, which showed significant agreement ($\tau = 0.749$, $P = .000$). For only 15 (22.7%) patients did T2-weighted imaging show hyperintense focal lesions, different from focal cortical contusions (61 total lesions; median, 0 lesions; range, 0–10 lesions). These foci were most often also seen as hyperintense signal intensities on the T2*-weighted images. Significantly fewer focal T2 hyperintensities than T2* hypointensities were seen (Wilcoxon matched-pairs signed rank test, $P = .0000$).

Figure 1 and Table 3 summarize the data concerning the frequency of specific lesion patterns and sites. Because traumatic microbleeds were more often and more easily detectable on the T2*-weighted images, only those data are shown. Isolated traumatic microbleeds were observed in 11 (16.7%) patients. Traumatic microbleeds were located mainly in the frontal (total microbleeds, 301.5; median, 0.75 microbleeds; range, 0–28 microbleeds) and temporal (total microbleeds, 115.5; median, 0 microbleeds; range, 0–19 microbleeds) lobes. The white matter of the superior frontal gyrus was most often affected (Fig 2). Furthermore, the traumatic microbleeds were situated mainly at the gray matter-white matter border (Fig 3). The traumatic microbleeds were located more often next to the crowns than close to the base of the gyral stalks. Lesions (focal cortical contusions and traumatic microbleeds) were situated in only one hemisphere in each of 10 patients (in the right in five, 7.6%; in the left in five, 7.6%) and in both hemispheres in each of 36 (54.5%). In the corpus callosum in 14 (21.2%) patients, a total of 32 traumatic microbleeds were found (median, 0 microbleeds; range, 0–7.5 microbleeds) (Fig 4). By contrast, in only two (3%) patients, a total of seven T2-hyperintense lesions of the corpus callosum were seen. Callosal traumatic microbleeds were restricted to the posterior parts (ie, splenium) in eight patients (12.1% or 57.1% of callosal lesions). In six (9.1%) patients, involvement of the brain stem was observed, mostly of the superior cerebellar peduncle (Fig 5). Focal cortical contusions

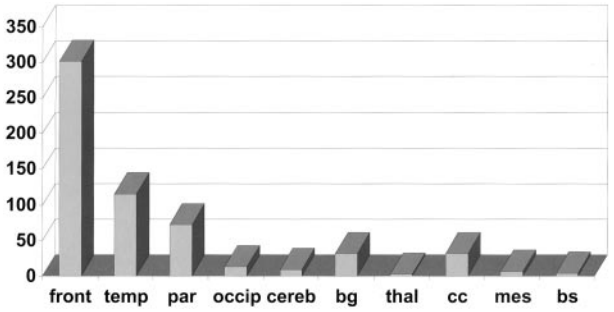

FIG 1. Frequency and site of traumatic microbleeds according to 10 brain areas. Shown is the total number of traumatic microbleeds in each brain area (*front*, frontal lobe; *temp*, temporal lobe; *par*, parietal lobe; *occip*, occipital lobe; *cereb*, cerebellum; *bg*, basal ganglia; *thal*, thalamus; *cc*, corpus callosum; *mes*, mesencephalon; *bs*, brain stem).

TABLE 3: Frequency of specific lesion patterns and sites

	Number	Percent
MR imaging-negative	10	15.2
Concerning TMBs	20	30.3
TMBs/DAI		
None or nonisolated	55	83.3
Isolated	11	16.7
FCC	37	56
Isolated	13	19.7
Side of lesion(s)		
Right	5	7.6
Left	5	7.6
Both	36	54.5
Corpus callosum lesion		
None	52	78.8
Anterior	4	6.1
Posterior	8	12.1
Diffuse	2	3.0
Brain stem involvement	6	9.1
Other traumatic lesions (isolated or in combination)		
Traumatic hematomas	2	3
Gliding contusions	6	9
SAB	7	10.6
SDH	6	9
EDH	5	7.6
Ischemic lesions	3	4.5
Residues		
Atrophy/hydrocephalus	7	10.6

Note.—TMBs indicates traumatic microbleeds; DAI, diffuse axonal injury; FCC, focal cortical contusion; SAB, subarachnoid hemorrhage; SDH, subdural hematoma; EDH, epidural hematoma.

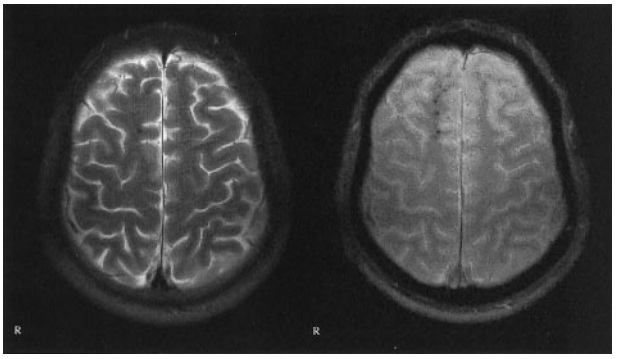

FIG 2. Images of a 20-year-old man who was a passenger in a traffic accident in May 1999; he had not been wearing a seat belt. Multiple traumatic microbleeds are shown in the white matter of the right superior frontal gyrus. *Left*, T2-weighted image; *right*: T2*-weighted image. Axial view sections obtained from the identical location. Multiple traumatic microbleeds, which are clearly shown on the T2*-weighted gradient-echo images, are not depicted on the T2-weighted MR images. Note that no T2-hyperintense foci are seen. GCS score, 3; GOS score, 5.

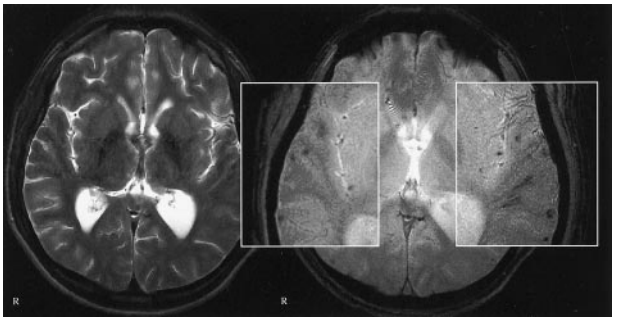

FIG 3. Images of a 22-year-old man who was the driver of a car that collided with a truck in June 1999. Multiple traumatic microbleeds are shown at the gray matter-white matter border. *Left*, T2-weighted image; *right*, T2*-weighted image. Images were obtained in the same plane. GCS score, 5; GOS score, 4.

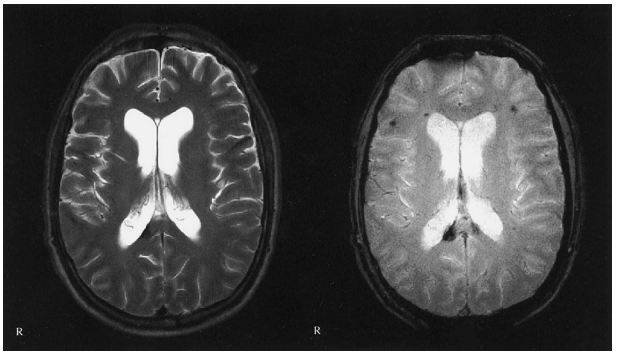

FIG 4. Images of a 42-year-old man who was a passenger in a traffic accident in September 2000. Traumatic microbleeds are shown in the posterior corpus callosum. *Left*, T2-weighted image; *right*, T2*-weighted image. Note the additional traumatic microbleeds in the left side of the splenium and at the gray matter-white matter border of the frontal lobes, which are not visible on the T2-weighted images. No T2-hyperintense callosal lesions are seen. GCS score, 3; GOS score, 4.

were observed in 37 patients; in 13 (19.7% or 35.1% of focal cortical contusions), they were isolated. Other specified intra- or extra-axial traumatic lesions were detected in 29 (43.7%) patients. Long-term residues of traumatic brain injury, such as brain atrophy and hydrocephalus, were observed in seven (10.6%) patients.

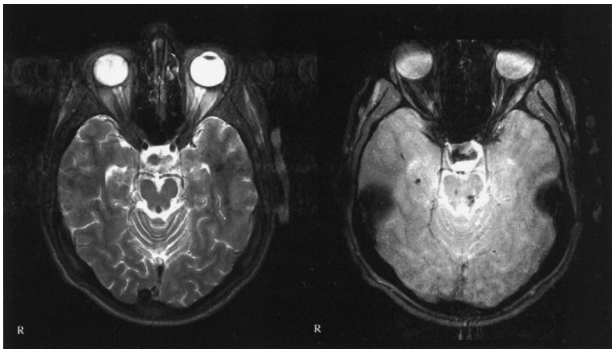

FIG 5. Images of a 39-year-old woman who fell off a horse in July 1996. Traumatic microbleeds are shown in the left rostral brain stem (superior cerebellar peduncle), which is a preferential site for diffuse axonal injury. The nearly symmetrical additional larger dark areas are artifacts from the petrous bone. *Left*, T2-weighted image; *right*, T2*-weighted image. GCS score, 14; GOS score, 6.

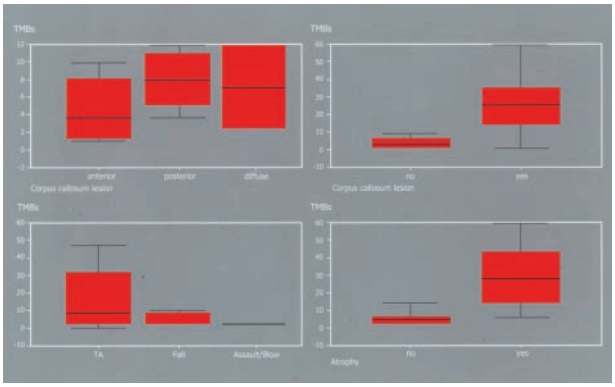

FIG 6. Relationships between number and site of traumatic microbleeds and clinical and imaging parameters. *Top left*, relationship of number of traumatic microbleeds to site of a callosal lesion ($P = .0001$). *Top right*, relationship of total number of traumatic microbleeds to the existence of a callosal lesion in general ($P = .0000$). *Bottom left*, relationship of total number of traumatic microbleeds to cause of injury (*TA*, traffic accident; $P = .0028$). *Bottom right*, relationship of total number of traumatic microbleeds to existence of inner brain atrophy ($P = .0020$).

Relationships between MR Imaging Findings and Clinical Parameters

Figure 6 shows the derived inter-relationships between the main clinical data and the findings on the T2*-images (for the original data, see also Table 4 on the journal's web site at www.ajnr.org). After correction for multiple testing, no correlation was observed between the time interval from trauma to MR imaging and the total number of traumatic microbleeds detected by T2*-weighted gradient-echo imaging ($r_s = -0.29$, $P = .02$). Regarding the cause of traumatic brain injury, a significant gradient was observed for traffic accident over fall to assault/blow. Most traumatic microbleeds were observed in victims of traffic accidents ($P = .0028$, Kruskall-Wallis analysis

TABLE 4: Tested inter-relations between the clinical parameters and the neuroradiologic data

Relationship Tested	Median (Range)	Rs	*P*
T2* latency (TBI–MR imaging)		−0.286	0.020
T2* type of TBI			0.7211
Closed	4.0 (0–61)		
Open	2.0 (0–52.5)		
T2* cause of TBI			0.0028*
Traffic accident	5.5 (0–61)		
Fall	2.5 (0–34)		
Blow/assault	0 (0–5)		
T2* multiple injuries			0.2481
No	3.5 (0–52.5)		
Yes	5.5 (0–61)		
T2* atrophy/hydrocephalus			0.0020*
No	3.5 (0–45.5)		
Yes	28 (4–61)		
T2* isolated TMBs			0.1266
No	3.5 (0–52.5)		
Yes	4.5 (0.5–61)		
T2* corpus callosum lesion			0.0000*
No	2.0 (0–34)		
Yes	26.0 (1.5–61)		
T2* GCS score (n = 62) for total hypo foci		−0.427	0.000*
T2* GCS score (n = 62) for hypo foci in corpus callosum		−0.428	0.000*
Corpus callosum lesion GCS score (n = 62)			0.002*
No	6 (3–15)		
Yes	4 (3–14)		
T2* GOS score for total hypo foci		−0.062	0.618
T2* GOS score for hypo foci in corpus callosum		−0.103	0.408
Corpus callosum lesion GOS score			0.3674
No	5 (3–8)		
Yes	5 (3–8)		
Isolated TMBs GOS score			0.8856
No	5 (3–8)		
Yes	5 (4–7)		
Isolated FCC GOS score			0.1724
No	5 (3–8)		
Yes	4 (3–6)		

Note.—Rs indicates Spearman rank correlation coefficient; T2*, T2*-weighted MR imaging; TBI, traumatic brain injury; TMBs, traumatic microbleeds; GCS, Glasgow Coma Scale; hypo, hypointense; GOS, Glasgow Outcome Scale; FCC, focal cortical contusion.

of variance). Patients with possible long-term residues of traumatic brain injury (atrophy/hydrocephalus) had significantly more traumatic microbleeds shown on the T2*-images than those without (P = .0020, Mann-Whitney U test). The same correlation was observed for patients with involvement of the corpus callosum (P = .0000, Mann-Whitney U test). Significant correlations were observed between the GCS score and the total number of traumatic microbleeds in each patient, the number of traumatic microbleeds in the corpus callosum, and the presence of a callosal lesion in general (P = .000/0.000, Spearman rank correlation; P = .0000, Mann-Whitney U test). No correlations could be detected between the morphologic findings on the T2*-images and the GOS scores. Cross-correlation between the GCS and the GOS scores showed no significant correlation (P = .312, Spearman rank correlation). Regarding outcome, it made no difference whether focal cortical contusions and/or traumatic microbleeds occurred in isolation or in combination with other lesion patterns. No correlations could be shown between the presence of T2-hyperintense focal lesions and the parameters of the GCS and GOS.

Discussion

Our hypotheses can be answered as follows: 1) T2*-weighted gradient-echo imaging shows more focal traumatic lesions other than focal cortical contusions than do T1- and T2-weighted MR imaging of patients with chronic traumatic brain injury; 2) a negative interrelation exists between the GCS score as a parameter of injury severity and the occurrence and amount of traumatic microbleeds, but neither their number nor site reflect overall long-term clinical outcome, as measured by the extended GOS.

Previous MR Imaging Studies of Traumatic Brain Injury in Comparison with Our Study

Most MR imaging studies have reported nonhemorrhagic foci (ie, hyperintense on T2-weighted images) as the neuroradiologic correlates of diffuse axonal injury (6, 21, 24). Gentry et al (21) define these lesions as mainly T2-hyperintense, diffuse, small (5–15 mm), focal abnormalities limited to white matter tracts. T2-hyperintense signals are unspecific (39). Periventricular hyperintensities are reported to be present in 74% of young normal persons and in 89% of elderly normal persons. The frequency of subcortical lesions in these two groups is reported to be 6% and 39%, respectively (40). It is therefore questionable whether all the reported hyperintensities represent sites of axonal shear injury. A size of >5 mm does not correspond to the existing neuropathologic descriptions of diffuse axonal injury, with which focal lesions usually do not measure more than 3 to 5 mm but extend over an anteroposterior distance of several centimeters (10, 11, 13, 19). As previously noted by Yanagawa et al (9), possible asymptomatic cerebral infarctions may comprise one cause of T2 hyperintensities, especially if elderly patients are included in a study. During the acute stage of traumatic brain injury, focal edema might be another cause of T2-hyperintense signal intensity changes.

Other inconsistencies concerning the results of the previous studies are now considered in more detail. In their study of acute traumatic callosal lesions, Gentry et al (38) found a high incidence of intraventricular hemorrhage in association with callosal injury, which is explained by the rich vascularity of the corpus callosum. Nevertheless, the authors state that the

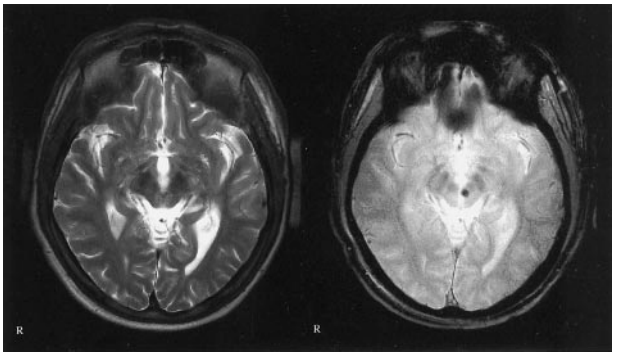

FIG 7. Images of a 37-year-old man who was a pedestrian in a traffic accident in January 1992; he was hit by an automobile while under the influence of alcohol. Traumatic microbleed is shown in the left midbrain, adjacent to the red nucleus, 99 months after traumatic brain injury. *Left*, T2-weighted image; *right*, T2*-weighted image. GCS score, 4; GOS score, 4.

callosal lesions themselves were most commonly nonhemorrhagic, which does not seem reasonable. Mittl et al (6) reported T2-hyperintense foci of shear injury in three (15%) of 20 patients. A closer review of the patients' data reveals two arguments against this view. All three patients had lost consciousness after assaults. According to the neuropathologic literature (10, 11), although assaults can cause traumatic brain injury, they are usually not associated with diffuse axonal injury. Furthermore, none of the lesions were located in the corpus callosum, which is a preferential site of diffuse axonal injury (10, 11, 19).

We found significantly more hypointense foci on the T2*-weighted images than hyperintense foci on the T2-weighted images. The appearance of T2*-hypointense foci was correlated with traffic accidents as the major cause of diffuse axonal injury of the human brain (10–12, 18). Most of the lesions were small (1–5 mm), multiple, and bilateral. They were predominantly localized in discrete brain areas—particularly in the white matter of the superior frontal gyrus, at the gray matter-white matter border of the frontal and temporal lobes, and in the corpus callosum—all of which are preferential sites for neuropathologically proved diffuse axonal injury. Lesion size corresponds closely to the neuropathologic characterization of tissue tear hemorrhages (10, 11, 13, 19). Because of the absence of a significant relationship between the presence of traumatic microbleeds and the latency of MR imaging, the visibility of diffuse axonal injury-related injury on T2*-images seems to be time independent. Even >90 months after traumatic brain injury, traumatic microbleeds could clearly be shown (Fig 7). Hematoma resorption can therefore not be responsible for the discrepancies between the previous studies and ours, especially considering that the previous studies were conducted of the acute stages of traumatic brain injury.

Almost all previous MR imaging studies have been performed at field strengths up to 1.5 T. Our study is the first that used a 3-T MR imaging system. Because the T2* signal intensity loss depends on magnetic field strength (1, 6, 7), the hemorrhagic component of diffuse axonal injury might have been underestimated at 1.5 T and by T2-imaging only. However, it was not our purpose to prove the superiority of 3 T, which of course would require a direct comparison with 1.5 T.

We do not assume that the lower incidence of hyperintense lesions on the T2-weighted images in our study might have been due to increased susceptibility at 3 T. Although increased susceptibility at 3 T may cause some additional dephasing that might mask an otherwise hyperintense focus on the T2-weighted images, such dephasing would necessitate a dephasing in the T2*-weighted images as well. Thus, although this effect might cause the "masking" of a focus from the T2-weighted images, such dephasing must be significant and so is more than likely to cause the foci to appear as hypointense foci on the T2*-weighted image. Such behavior, however, would require that these foci have both a freer water environment (to allow a longer T2 for the hyperintense signal intensity) and a minor susceptibility component (insufficient to dephase the signal intensity at 1.5 T but sufficient at 3 T). It seems unlikely that these two would occur simultaneously, with the correct balance of effects on the MR signal intensity, over a significant number of lesions.

Other Causes of T2-Hypointense Signals*

The overall incidence of small hypointense lesions on T2*-weighted gradient-echo images in neurologically healthy adults is reported to be 3.1%, and they are closely related to arterial hypertension (34). Because of the low prevalence of chronic arterial hypertension (0.66%), diabetes mellitus (0%), or stroke (0%) in our patient population, the frequency of incidental T2* hypointensities should not interfere with our results.

It must be noted that the signal intensity loss on T2*-weighted images is not specific for hemorrhage and can be caused by calcifications, ferritin, air in sinuses or mastoid bone, and paramagnetic contrast agents (1, 4, 5). Considering that shear injuries are typically not situated on the cortical surface or at contusion sites close to the skull base, this nonspecificity is not a main limitation for the evaluation of diffuse axonal injury. Calcifications are usually located in the basal ganglia, which are the site of basal ganglia hematomas (41). These seem to be related to diffuse axonal injury and are characterized by a poor outcome (10, 11, 39). Diffuse vascular injury is also distinguishable based on its very poor prognosis. Usually patients die within a short interval after injury (42). The presence of these conditions among our patient population is very unlikely. Other causes of multiple cerebral hemorrhages could be fat embolism and medical complications after traumatic brain injury, such as hematologic disorders or sepsis or side effects of medical therapy. Although such complications have not been reported among our patient population, their relevance remains unclear.

Functional Outcome

It is noteworthy that there is neither a correlation between the total number of lesions detected by T2*-weighted gradient-echo imaging and the GOS nor between the GOS and any other of the imaging parameters, such as evidence of a callosal lesion or isolated traumatic microbleeds/diffuse axonal injury. This is in contrast to the study presented by Yanagawa et al (9), which was conducted of the acute stage of traumatic brain injury and which does not differentiate between diffuse axonal injury-related lesions and focal cortical contusions. Another explanation for this discrepancy might be that in the latter study, data for the GOS were collected 3 months after traumatic brain injury. However, the GOS and its extended version are validated for outcome measurement not before 6 months after traumatic brain injury (26, 43). In the study presented by Pierallini et al (8), a significant correlation was shown between clinical scores (GCS, GOS) and total lesion volume on fluid-attenuated inversion recovery but not T2*-weighted images.

Diffuse axonal injury is usually related to general poor clinical status (44). Our data indicate that this seems to be true only for the acute stage of traumatic brain injury. A strong correlation existed between the number of traumatic microbleeds and the GCS scores, which reflects the potential of diffuse axonal injury to cause severe coma (44, 45). On the other hand, because of the lack of a correlation with the GOS scores it seems very likely that diffuse axonal injury is not inevitably related to poor long-term outcomes. Already, the findings presented by Wilson et al (45) question the importance of diffuse axonal injury in determining outcome. The GCS itself is not a sufficient outcome predictor (27, 45). Because cognitive dysfunction seems to be more responsible for overall disability after traumatic brain injury than do motor deficits (26), more detailed neuropsychologic testing is needed for clarification. The recent studies presented by Wallesch et al (46, 47) are in line with our results. The authors state that diffuse axonal injury causes mainly transient neuropsychologic deficits. A limitation of these studies is the use of cranial CT for the diagnosis of diffuse axonal injury.

Conclusion

During the chronic stage of traumatic brain injury, T2*-weighted gradient-echo imaging at high field strength is superior to T1- and T2-weighted MR imaging in the detection of lesions suspicious of diffuse axonal injury. Based on the signal intensity characteristics on T2*-weighted gradient-echo images, most of these lesions are hemorrhagic. Their visibility on T2*-weighted gradient-echo images is time independent, which allows recognition during the chronic stage of traumatic brain injury. Evidence of diffuse axonal injury is thought to be of relevance regarding rehabilitative treatment, patient prognosis, and medical diagnostic certainty; however, the lack of correlation between number and site of traumatic microbleeds and an overall long-term clinical outcome parameter such as the GOS questions this view. The clinical and prognostic implications of our findings will therefore have to be examined further by correlation with the results of neuropsychologic testing.

Acknowledgments

Statistical advice and review were provided by J. Forberg, PhD, Department of Medical Information Science, Statistics and Epidemiology, University of Leipzig. We thank S. Vogel (medical student) for collecting some of the data for the calculation of the GCS and GOS scores.

References

1. Atlas SW, Mark AS, Grossman RI, Gomori JM. **Intracranial haemorrhage: gradient-echo MR imaging at 1.5 T.** Comparison with spin-echo imaging and clinical applications. *Radiology* 1988;168:803–807
2. Bradley WG Jr. **MR appearance of hemorrhage in the brain.** *Radiology* 1993;189:15–26
3. Fazekas F, Kleinert R, Roob G, et al. **Histopathologic analysis of foci of signal loss on gradient-echo T2*-weighted MR images in patients with spontaneous intracerebral hemorrhage: evidence of microangiopathy-related microbleeds.** *AJNR Am J Neuroradiol* 1999;20:637–642
4. Edelman RR, Johnson K, Buxton R, et al. **MR of hemorrhage: a new approach.** *AJNR Am J Neuroradiol* 1986;7:751–756
5. Roob G, Kleinert R, Seifert T, et al. **MRI evidence of cerebral microbleeds: comparative histopathologic data and possible clinical implications.** *Nervenarzt* 1999;70:1082–1087
6. Mittl RL, Grossman RI, Hiehle JF, et al. **Prevalence of MR evidence of diffuse axonal injury in patients with mild head injury and normal head CT findings.** *AJNR Am J Neuroradiol* 1994;15:1583–1589
7. Gomori JM, Grossman RI, Goldberg HI, Zimmerman RA, Bilaniuk LT. **Intracranial haematomas: imaging by high-field MR.** *Radiology* 1985;157:87–93
8. Pierallini A, Pantano P, Fantozzi LM, et al. **Correlation between MRI findings and long-term outcome in patients with severe brain trauma.** *Neuroradiology* 2000;42:860–867
9. Yanagawa Y, Tsushima Y, Tokumaru A, et al. **A quantitative analysis of head injury using T2*-weighted gradient-echo imaging.** *J Trauma* 2000;49:272–277
10. Graham DI, Gennarelli TA. **Trauma.** In: Graham DI, Lantos PI, eds. *Greenfield's Neuropathology.* 6th ed. London: Arnold; 1997: 197–262
11. Graham DI, Gennarelli TA. **Pathology of brain damage after head injury.** In: Cooper PR, Golfinos JG, eds. *Head Injury.* 4th ed. New York: McGraw-Hill; 2000:133–153
12. Meythaler JM, Peduzzi JD, Eleftheriou E, Novack TA. **Current concepts: diffuse axonal injury-associated traumatic brain injury.** *Arch Phys Med Rehabil* 2001;82:1461–1471
13. Gennarelli TA, Thibault LE, Adams JH, et al. **Diffuse axonal injury and traumatic coma in the primate.** *Ann Neurol* 1982;12:564–574
14. Gentleman SM, Nash MJ, Sweeting CJ, Graham DI, Roberts GW. **β-Amyloid precursor protein (β-APP) as a marker of diffuse axonal injury after head injury.** *Neurosci Lett* 1993;160:139–144
15. Sherriff FE, Bridges LR, Sivaloganathan S. **Early detection of axonal injury after human head trauma using immunocytochemistry for beta-amyloid precursor protein.** *Acta Neuropathol (Berl)* 1994;87:55–62
16. Leclercq PD, McKenzie JE, Graham DI, Gentleman SM. **Axonal injury is accentuated in the caudal corpus callosum of head-injured patients.** *J Neurotrauma* 2001;18:1–19
17. Povlishock JT. **Traumatically induced axonal injury: pathogenesis and pathobiological implications.** *Brain Pathol* 1992;2:1–12
18. Maxwell WL, Povlishock JT, Graham DL. **A mechanistic analysis of nondisruptive axonal injury: a review.** *J Neurotrauma* 1997;14: 419–440
19. Adams JH, Doyle D, Ford I, Gennarelli TA, Graham DI, McLellan DR. **Diffuse axonal injury in head injury: definition, diagnosis and grading.** *Histopathology* 1989;15:49–59
20. Yokota H, Kurokawa A, Otsuka T, Kobayashi S, Nakazawa S. **Significance of magnetic resonance imaging in acute head injury.** *J Trauma* 1991;31:351–357

21. Gentry LR, Godersky JC, Thompson B. **MR imaging of head trauma: review of the distribution and radiopathologic features of traumatic lesions.** *AJR Am J Roentgenol* 1988;150:663–672
22. Kampfl A, Schmutzhard E, Franz G, et al. **Prediction of recovery from post-traumatic vegetative state with cerebral magnetic resonance imaging.** *Lancet* 1998;351:1763–1767
23. Gentry LR. **Imaging of closed head injury.** *Radiology* 1994;191:1–17
24. Gentry LR, Godersky GC, Thompson B, Dunn VD. **Prospective comparative study of intermediate-field MR and CT in the evaluation of closed head trauma.** *AJNR Am J Neuroradiol* 1988;150:673–682
25. Teasdale G, Jennett B. **Assessment of coma and impaired consciousness: a practical scale.** *Lancet* 1974;2:81–84
26. Jennet B, Snoeck J, Bond MR, Brooks N. **Disability after severe head injury: observations on the use of Glasgow Outcome Scale.** *J Neurol Neurosurg Psychiatry* 1981;44:285–293
27. Katz DI, Alexander MP. **Traumatic brain injury: predicting course of recovery and outcome for patients admitted to rehabilitation.** *Arch Neurol* 1994;51:661–670
28. Norris DG. **Reduced power multislice MDEFT imaging.** *J Magn Reson Imaging* 2000;11:445–451
29. Roob G, Schmidt R, Kapeller P, Lechner A, Hartung HP, Fazekas F. **MRI evidence of past cerebral microbleeds in a healthy elderly population.** *Neurology* 1999;52:991–997
30. Greenberg SM, Finklestein SP, Schaefer PW. **Petechial hemorrhages accompanying lobar hemorrhage: detection by gradient-echo MRI.** *Neurology* 1996;46:1751–1754
31. Greenberg SM, O'Donnell HC, Schaefer PW, Kraft E. **MRI detection of new hemorrhages: potential marker of progression in cerebral amyloidangiopathy.** *Neurology* 1999;53:1135–1141
32. Kinoshita T, Okudera T, Tamura H, Ogawa T, Hatazawa J. **Assessment of lacunar hemorrhage associated with hypertensive stroke by echo-planar gradient-echo T2*-weighted MRI.** *Stroke* 2000;31:1646–1650
33. Hermier M, Nighoghossian N, Derex L, et al. **MRI of acute post-ischemic cerebral hemorrhage in stroke patients: diagnosis with T2*-weighted gradient-echo sequences.** *Neuroradiology* 2001;43:809–815
34. Tsushima Y, Tanizaki Y, Aoki J, Endo K. **MR detection of micro-hemorrhages in neurologically healthy adults.** *Neuroradiology* 2002;44:31–36
35. Cohen JA. **Coefficient of agreement for nominal scales**. *Educ Psychol Meas* 1960;20:37–46
36. Fleiss JL. *Statistical Methods for Rates and Proportions.* 2nd ed. New York: Wiley; 1981:321
37. Kendall MG, Gibbons JD. *Rank Correlation Methods.* 5th ed. New York: Oxford University Press; 1990:260
38. Gentry LR, Thompson B, Godersky JC. **Trauma to the corpus callosum: MR features.** *AJNR Am J Neuroradiol* 1988;9:1129–1138
39. Munoz DG, Hastak SM, Harper B, Lee D, Hachinski VC. **Pathologic correlates of increased signals of the centrum ovale on magnetic resonance imaging.** *Arch Neurol* 1993;50:492–497
40. Bowen BC, Barker WW, Loewenstein DA, Sheldon J, Duara R. **MR signal abnormalities in memory disorder and dementia.** *AJR Am J Roentgenol* 1990;154:1285–1292
41. Adams JH, Doyle D, Graham DI, et al. **Deep intracerebral (basal ganglia) haematomas in fatal non-missile head injury in man.** *J Neurol Neurosurg Psychiatry* 1986;49:1039–1043
42. Tomlinson BE. **Brain-stem lesions after head injury**. *J Clin Pathol Suppl (R Coll Pathol)* 1970;4:154–165
43. Jennett B, Bond M**. Assessment of outcome after severe brain damage**. *Lancet* 1975;1: 480–484
44. Adams JH, Graham DI, Gennarelli TA, Maxwell WL. **Diffuse axonal injury in non-missile head injury.** *J Neurol Neurosurg Psychiatry* 1991;54:481–483
45. Wilson JT, Hadley DM, Wiedmann KD, Teasdale GM. **Neuropsychological consequences of two patterns of brain damage shown by MRI in survivors of severe head injury.** *J Neurol Neurosurg Psychiatry* 1995;59:328–331
46. Wallesch CW, Curio N, Galazky I, Jost S, Synowitz H. **The neuropsychology of blunt head injury in the early postacute stage: effects of focal lesions and diffuse axonal injury.** *J Neurotrauma* 2001;18:11–20
47. Wallesch CW, Curio N, Kutz S, Jost S, Bartels C, Synowitz H. **Outcome after mild-to-moderate blunt head injury: effects of focal lesions and diffuse axonal injury.** *Brain Inj* 2001;15:401–412